Title

Functional characterization and molecular cloning of the K+-dependent Na+/Ca2+ exchanger in intact retinal cone photoreceptors.

Journal

The Journal of general physiology, 129(1)

ISSN

0022-1295

Authors

Paillart, Christophe
Winkfein, Robert J
Schnetkamp, Paul PM
et al.

Publication Date

2007

DOI

10.1085/jgp.200609652

Peer reviewed

Functional Characterization and Molecular Cloning of the K^+-dependent Na^+/Ca^{2+} Exchanger in Intact Retinal Cone Photoreceptors

Christophe Paillart,[1] Robert J. Winkfein,[2] Paul P.M. Schnetkamp,[2] and Juan I. Korenbrot[1]

[1]Department of Physiology, School of Medicine, University of California San Francisco, San Francisco, CA 94143
[2]Department of Physiology and Biophysics, Hotchkiss Brain Institute, Faculty of Medicine, University of Calgary, Calgary, Alberta, T2N 4N1, Canada

Light-dependent changes in cytoplasmic free Ca^{2+} are much faster in the outer segment of cone than rod photoreceptors in the vertebrate retina. In the limit, this rate is determined by the activity of an electrogenic Na^+/Ca^{2+} exchanger located in the outer segment plasma membrane. We investigate the functional properties of the exchanger activity in intact, single cone photoreceptors isolated from striped bass retina. Exchanger function is characterized through analysis both of the electrogenic exchanger current and cytoplasmic free Ca^{2+} measured with optical probes. The exchanger in cones is K^+ dependent and operates both in forward and reverse modes. In the reverse mode, the K^+ dependence of the exchanger is described by binding to a single site with $K_{1/2}$ about 3.6 mM. From the retina of the fish we cloned exchanger molecules bassNCKX1 and bassNCKX2. BassNCKX1 is a single class of molecules, homologous to exchangers previously cloned from mammalian rods. BassNCKX2 exists in four splice variants that differ from each other by small sequence differences in the single, large cytoplasmic loop characteristic of these molecules. We used RT-PCR (reverse transcriptase polymerase chain reaction) of individual cells to identify the exchanger molecule specifically expressed in bass single and twin cone photoreceptors. Each and every one of the four bassNCKX2 splice variants is expressed in both single and twin cones indistinguishably. BassNCKX1 is not expressed in cones and, by exclusion, it is likely to be an exchanger expressed in rods.

The Journal of General Physiology

INTRODUCTION

In retinal rod and cone photoreceptors, the free concentration of cGMP and Ca^{2+} in the outer segment cytoplasm is high in the dark and decreases upon illumination to an extent and at a rate dependent on light intensity. The decrease in cGMP is caused by light-dependent activation of phophodiesterase, an enzyme that hydrolyzes the cyclic nucleotide and is the last in a cascade of successive biochemical reactions initiated by photoexcitation of the visual pigment (for reviews see Burns and Baylor, 2001; Ebrey and Koutalos, 2001; Burns and Arshavsky, 2005). The decrease in Ca^{2+} is caused by active transport of the cation out of the outer segment by a Na^+/Ca^{2+} exchanger (for review see Schnetkamp, 2004). In the dark, Ca^{2+} continuously enters rod and cone outer segment through open cyclic GMP-gated ion channels (CNG channels) and exits via the Na^+/Ca^{2+} exchanger. Illumination causes a decrease in cytoplasmic cGMP, CNG channels close and Ca^{2+} influx declines. The decrease in influx, in the presence of continuing active Ca^{2+} efflux via the exchanger (Yau and Nakatani, 1985; Hodgkin et al., 1987; Miller and Korenbrot, 1987), results in a light-dependent fall in cytoplasmic free Ca^{2+} (Gray-Keller and Detwiler, 1994; McCarthy et al., 1996; Sampath et al., 1999). Under experimental conditions designed to block both Ca^{2+} influx and efflux in the outer segment, illumination sufficiently bright to bleach visual pigment also causes a slow increase in cytoplasmic Ca^{2+} of unknown function and possibly associated with release from intracellular buffers (Fain et al., 2001; Cilluffo et al., 2004).

The time course of the light-dependent decrease in cytoplasmic Ca^{2+} is remarkably different in rod and cone outer segments. In rods, the Ca^{2+} decline upon instantaneous closure of all active CNG channels is well described by the weighted sum of two exponential processes (gecko, Gray-Keller and Detwiler, 1994; toad, Miller and Korenbrot, 1987; frog, McCarthy et al., 1996). In nonmammalian species at room temperature, the fast process has a time constant in the range of 0.67 to 1.35 s, while the slow one has a time constant in the range 5.3 to 6.7 s. In cones, the decrease in Ca^{2+} under comparable conditions is also well described by the weighted sum of fast and slow exponential processes, each of which is faster than those in rods; the fast exponential process has a time constant 0.14 to 0.16 s, while the time constant of the slow one is in the range of 1.5 to 3.5 s (tiger salamander, Sampath et al., 1999; zebrafish, Cilluffo et al., 2004). This difference in the rate of outer

Correspondence to Juan I. Korenbrot: juan.korenbrot@ucsf.edu

Abbreviations used in this paper: CNG, cyclic GMP-gated ion; RT-PCR, reverse transcriptase polymerase chain reaction.

segment Ca^{2+} clearance contributes to explain the known difference in photoresponse kinetics and sensitivity between the two receptor types (Korenbrot, 1995; Rebrik and Korenbrot, 2004).

It is firmly established that active Ca^{2+} efflux from rod outer segments in various species is mediated exclusively by the activity of a K^+-dependent Na^+/Ca^{2+} exchanger (Cervetto et al., 1989; Schnetkamp et al., 1989). Under physiological solutions, the transporter is electrogenic, one net inward positive charge per turnover, with a stoichiometry of 4 Na^+ (in) for 1 Ca^{2+} plus 1 K^+ (out) (Schnetkamp, 1989; Lagnado and McNaughton, 1991). It may operate in its normal forward mode (passive Na^+ influx, active Ca^{2+} efflux, net inward current) or a reverse mode (passive Na^+ efflux, active Ca^{2+} influx, net outward current) depending on the ionic gradients (for review see Schnetkamp, 2004). In cones, on the other hand, the active Ca^{2+} extrusion is Na^+ dependent (Nakatani and Yau, 1989), but whether it is also K^+ dependent has not been demonstrated in intact photoreceptors, although it has long been assumed to be the case (Hestrin and Korenbrot, 1990; Perry and McNaughton, 1991; Sampath et al., 1999). It is conceivable that rods and cones differ because the Na^+/Ca^{2+} exchanger in cones is K^+ independent. We demonstrate here that the Na^+/Ca^{2+} exchanger in cones is K^+ dependent and we characterize some of its physiological features.

While both rod and cone outer segments express K^+-dependent Na^+/Ca^{2+} exchangers, the molecular mechanisms that explain the difference in Ca^{2+} clearance rates between rods and cones are not known. Two simple alternatives are (1) that the same Ca^{2+} transporter molecule is expressed in both cell types at different surface densities, and (2) that different molecules are expressed in the two cell types. To resolve the query we must first know the molecular identity and functional features of the exchanger molecule in rods and cones. K^+-dependent Na^+/Ca^{2+} exchangers have been cloned and recognized to constitute a unique gene family named NCKX (human gene SLC24) that, to date, includes five isoforms (for review see Schnetkamp, 2004). NCKX1 protein was first purified from bovine retina (Cook and Kaupp, 1988) where it is expressed in rod outer segments, but not in those of cones (Kim et al., 1998). NCKX1 cDNA has been cloned from various mammalian retinas or eyes (human, Tucker et al., 1998; dolphin, Cooper et al., 1999; rat, Poon et al., 2000). NCKX1 mRNA is expressed in human and chicken rods (Prinsen et al., 2000). The Na^+/Ca^{2+} exchanger protein has not been purified from any cone photoreceptor. However, a retinal cDNA clone identified as NCKX2 is expressed (as mRNA) in ganglion cells and cone photoreceptors (human, Prinsen et al., 2002; chicken, Prinsen et al., 2000). Uncertainty on the molecular identity of the transporter in cones has been introduced by the recent finding that knocking out NCKX2 in mice (Li et al., 2006) seriously impairs neuronal function in the hippocampus, but does not appear to suppress cone transduction signals, at least not as detected in the flash response of the photopic electroretinogram, although a finer analysis of cone transduction in these animals is yet to be completed.

We report here the cloning and molecular characterization of NCKX1 and NCKX2 molecules in the striped bass retina. We use single cell reverse transcriptase polymerase chain reaction (RT-PCR) to determine the cellular origin of the cloned NCKX molecules. We find bassNCKX2 (in four splice variant forms) is specifically expressed in both single and twin cones and bassNCKX1 is not. BassNCKX1 is likely an exchanger in rods.

MATERIALS AND METHODS

Materials

Striped bass (*Morone saxatilis*) were received from a commercial supplier (Professional Aquaculture Services), maintained in an aquaculture facility under 14:10 L:D cycles and fed ad lib. The UCSF Committee on Animal Research approved protocols for the upkeep and sacrifice of the animals. Nifendipine was obtained from CalBiochem and bis-Fura2 from Molecular Probes.

Retinal Cell Dissociation

Fish were dark adapted for 50 min, killed in darkness, and their eyes enucleated under infrared illumination with the aid of an IR-sensitive TV camera and video monitor. Under bass Ringer's (Table I), the retina was separated from a hemissected eye and subjected to gentle proteolysis (collagenase and hyaluronidase 1 mg/ml each) for 5 min at room temperature. Enzymes and glucose were washed away by repeated exchange with enzyme-free Ringer's in which glucose was replaced by pyruvate (5 mM). Photoreceptors were isolated by mechanical trituration of the retina in the pyruvate-Ringer and collected by gentle aspiration of the resulting cell suspension (Miller and Korenbrot, 1993).

Solutions

The composition of extracellular and electrode-filling solutions is listed in Table I. The intracellular composition was taken to be the same as the electrode filling solutions. In general, electrode-filling solutions were of two classes: (1) SBIS (striped bass internal solution), designed to mimic the normal intracellular ionic composition and used to characterize the cone's photocurrents, and (2) NCKX-IS, designed to study the Na^+/Ca^{2+}, K^+ exchanger operating in reverse mode. These solutions were modified to include either 0.1 mM bis-Fura2 or 2 mM BAPTA titrated with $CaCl_2$ to yield 400 nM free Ca^{2+}. Ca^{2+}-buffered solutions were designed using WinMaxC software (www.stanford.edu/~cpatton).

Electrical Recording

The retinal cell suspension was transferred to an electrophysiological recording chamber held on an inverted microscope equipped with DIC contrast enhancement. The bottom of the chamber was a glass coverslip covalently coated with wheat germ agglutinin to which photoreceptors firmly adhered. After 10 min, the bathing solution in the chamber was exchanged with glucose-Ringer's containing 0.1 mg/ml BSA. The bath solution was intermittently exchanged throughout the experimental sessions.

TABLE I

Composition of Ionic Solutions

Extracellular solutions				Electrode-filling solutions			
	Photocurrent data		NCKX data	Photocurrent data		NCKX data	
	Na^+ Ringer's[a]	Li^+/HEDTA-Ringer's	Li^+-Ringer's	SBIS[e]		NCKX-IS[e]	
NaCl	143			K gluconate	115	gluconic acid	100
$NaHCO_3$	5			K aspartate	20	aspartic acid	20
$NaHPO_4$	5			KCl	20	KOH	10
KCl	2	2.5	Various in isoosmotic exchange for Li^+	$MgCl_2$	0.5[c]	NaOH	25
LiCl		157.5	160	$ATPNa_2$	3	TEACl[f]	35
TEACl		5	5	$GTPNa_3$	1	TMAOH[f]	92[d]
$MgCl_2$	1	0.5[b]	1				
$CaCl_2$	1	0.001[b]	0.1				
HEPES	10	10	10	MOPS	10	MOPS	10
Glucose	10						
pH	7.5	7.5	7.5		7.25		7.25
mOsM	310	310	310		305		305

Concentrations are all in mM.

[a]Ringer's also contained 1× minimum essential medium (MEM) vitamins and amino acids and 0.1 mg/ml BSA.

[b]To obtain the free concentrations listed, the solution contained total: HEDTA (2.5 mM), Mg^{2+} (2.5 mM), and Ca^{2+} (0.1 mM).

[c]Total Mg^{2+} (4 mM).

[d]As needed to attain final pH.

[e]Solutions were made free of multivalent cations by passing them over Chelex-100 resin before adding Mg^{2+} or nucleotides.

[f]Tetraethylammoniun (TEA), tetramethylammonium (TMA).

We measured membrane current at room temperature under voltage-clamp using tight-seal electrodes in the whole-cell mode. Electrodes were produced from aluminosilicate glass (Corning 1724, 1.5 × 1.1 mm od x id). Current were recorded with a patch clamp amplifier (Axopatch 1D; Axon Instruments). Analogue signals were low pass filtered through 8-pole Bessel filters (Frequency Devices) and digitized on line at twice the analogue rate (Digidata1322A and pClamp software; Axon Instruments). Analogue recording bandpass in photocurrent studies was 0–500 Hz, while it was 0–20 Hz when measuring reverse NCKX currents.

Light Stimulation

Stimuli were delivered through an epi-illumination system that used the microscope objective as its final lens (Nikon Fluor 40×/1.3 NA oil). The focused image of an adjustable aperture placed on the optical path limited illumination to a 50 μm diameter circle centered on the cell under study. Light was generated by a DC operated Tungsten source. Narrow band interference (10 nm bandwidth) and calibrated neutral density filters controlled light color and intensity, while stimulus duration was controlled with an electronically triggered electromechanical shutter (Vincent and Associates). The cross section of absorption of the bass single cone outer segment on its side is 1.91 μm^2. To generate 1-ms half-bandwidth light flashes, two shutters were placed in series and electronically controlled as needed. Light intensity was measured with a calibrated photodiode placed on the microscope stage at the same position as the cells (UDT Sensors, to measure monochromatic light intensity, or Industrial Fiber Optics photometer, to measure white light power).

Single Cell Superfusion

The electrophysiological recording chamber was free to rotate on the microscope stage. This allowed us to align the cone under investigation such that superfusing solutions flowed along its long axis and reduced the possibility that the flowing solution dislodged the cell. Superfusing solutions flowed from a 1 cm long, 300 μm ID polyimide capillary (PT Technologies, Vista, CA) placed with its tip ~300 μm from the cell under study and in the same vertical plane. The capillary was the exit port of a 6 input port micromanifold (Model MM-6, Warner Instruments, Hamden, CT). The identity and duration of the solutions superfusing cells under study were selected with electronic control valves (The Lee Company, Westbrook, CT) controlled with a programmable processor (Model MPS-2, WPI Instruments, Sarasota, FL).

Cytoplasmic Free Ca^{2+} in Single Cone Outer Segments

Individual cells were filled with bis-Fura2 (0.1 mM) by exchange/diffusion from the electrode filling solution. Single cell current and fluorescence intensity were measured simultaneously using an instrument previously described in detail (Ohyama et al., 2000). Fluorescence excitation at 380 nm (5 nm half-bandwidth) was limited to a 15-μm diameter circle centered on the cell under study by an aperture placed in the epi-illumination pathway. Emitted fluorescence was captured with a custom-designed water immersion miniature lens system (5 mm diameter, 0.6 NA, and 2.8 mm working distance) that focused the captured light onto the end of a single fiber optic. The fiber optic guided light onto a cooled photomultiplier tube (−20°C, Model R943; Hamamatsu) operated in photon counting mode (model SR400; Stanford Research Systems).

Data Analysis

Errors are presented as standard deviation. Selected mathematical functions were fit to experimental data with computer-aided nonlinear least square minimization algorithms (Origin Software, Origin Labs, Northampton, MA).

Screen of Bass Retinal cDNA Phagemid Library

RNA was purified from retinas isolated from light-adapted bass eyes. Freshly isolated tissue was immediately frozen under liquid nitrogen and total RNA recovered using guanidium isothiocyanate (Chomczynski and Sacchi, 1987). mRNA was separated using oligo-dT cellulose chromatography and a cDNA library was constructed

TABLE II

Sequence and Melting Temperature (Ta) of Primers Used in Single-Cell RT-PCR of Cone Photoreceptors To Determine the Cellular Expression of NCKX Homologues

Name	Sense	Sequence
bassNCKX2-specific primers		
SBX1	Forward	5′-GCACCCAAAGATGATGAGAAC-3′
SBX2	Reverse	5′-AGAGCCACAGAGGAAGGATG-3′
SBX3	Forward	5′-GACGAAGGTATGGGACGTTTC-3′
SBX3M	Forward	5′-CTCAGTGACGAAGGTATGGG-3′
SBX4	Reverse	5′-GCTTTTCTTGGTTGTGTCTGG-3′
SBX5	Forward	5′-GTGACGAAGGACGTTTCAAAGAG-3′
SBX7	Forward	5′-CAATGCCAATGGTGTAGCTG-3′
SBX7M	Forward	5′-TGCCAATGGTGTAGCTGATAAA-3′
bassNCKX1-specific primers		
SBX13	Forward	5′-TGAGGAGCACCATCTTCCA-3′
SBX14	Reverse	5′-CTCCTCCTCCTCTTCTTCTTCTTC-3′

The annealing temperature, Ta, was 55°C for each and every one of the primers.

in Lambda ZapII phagemid using standard protocols (Stratagene). The library consisted of $\sim 5 \times 10^7$ independent pfu.

The library was screened by low stringency hybridization to a probe consisting of the transmembrane regions of a double deletion bovine NCKX1 clone (ddNCKX1), as detailed elsewhere (Prinsen et al., 2000). Positive clones were excised into pBluescript and sequenced. Analysis of these sequences identified two distinct NCKX molecules, tentatively identified as bass NCKX1 and NCKX2 by sequence homology to known sequences. We cloned four distinct splice variants of the bassNCKX2 clone (2.1, 2.2, 2.3, and 2.6). Full-length bass NCKX1 and NCKX2 clones were recovered by RACE amplification using retinal mRNA as substrate (Cooper et al., 1999). In bass NCKX1 we introduced a myc epitope tag between amino acid residues 95 and 96. In bass NCKX2 we introduced the same epitope tag between amino acid residues 98 and 99.

Single Cell RT-PCR

Suspensions of isolated photoreceptors in bass Ringer's were produced as described above. In light, 50–200 μl of the cell suspension was deposited onto a small volume chamber held on an upright microscope equipped with DIC contrast enhancement. The bottom of the chamber was a glass coverslip. The solution in the chamber was thoroughly perfused with Ringer's to remove cellular debris, and, in addition, individual cells were locally superfused with Ringer's immediately before their collection. Local superfusion was achieved with a polyimide-coated quartz capillary (ID 150 μm) positioned with its tip ~300 μm away from the cell. Under microscopic observation, individual single and twin photoreceptor cells were collected using suction micropipettes maneuvered with a micromanipulator. The micropipettes were fabricated from Corning 7052 glass capillary tubing (1.5/1.0 mm od/id) with a tip diameter only slightly larger than the width of solitary cells (8 μm for single and 14 μm for twin cones).

Individual cone photoreceptors were collected in the least possible volume (tens of picoliters). The suction micropipette was withdrawn from the chamber and its contents expelled under positive pressure into a 0.6-ml plastic tube containing reagents for immediate synthesis of cDNA using Sensiscript reverse transcriptase (QIAGEN) and Oligo (dT)12–18 as primer (Invitrogen), as described elsewhere (Paillart et al., 2006). After 1 h at 37°C, cDNA synthesis was terminated by 5 min incubation at 93°C. Samples were then stored at −80°C.

We performed two rounds of PCR amplification using HotStar Taq DNA polymerase (QIAGEN) in a final 50-μl volume. 4 or 5 μl of cell cDNA was used as template in the first round PCR, and 1 μl of the resulting product was used in the second round. The HotStar Taq DNA polymerase was initially activated at 95°C for 15 min. Typically, we used 30 PCR cycles, each consisting of 30-s periods at 94°C, 30 s at the appropriate annealing temperatures (Ta), and 1 min at 72°C. In the final cycle, the 72°C step was sustained for 11 min. PCR products were size separated by horizontal electrophoresis in 2% agarose gels. Discrete bands were excised, DNA recovered (QIAquick kit; QIAGEN) and sequenced.

The sequence and melting temperature (Ta) of primers used to specifically identify the expression of bass NCKX1 and the various slice variants of bass NCKX2 are listed in Table II. As positive control for the efficiency of the RT-PCR process, we assayed each cell sample for the expression of β subunits of the cone CNG channel (bass CNGB3) using the SB3/SB2 primers (Table II) in both PCR rounds, as detailed elsewhere (Paillart et al., 2006).

RESULTS

Previous research has demonstrated that active Ca^{2+} removal from the cone photoreceptor outer segments depends on the activity of a Na^+/Ca^{2+} exchanger (Nakatani and Yau, 1989). To investigate the properties of this active transporter, its potential dependence on K^+ ions, and its molecular structure we characterized Na^+/Ca^{2+} exchange in intact single cones isolated from striped bass retina. These are relatively large cells amenable to both physiological (Miller and Korenbrot, 1993) and molecular biology investigation (Paillart et al., 2006).

Na^+/Ca^{2+} Exchanger Activity (NCKX) in Bass Single Cone Photoreceptors

We measured membrane currents under voltage clamp using tight-seal electrodes filled with a solution designed to mimic normal intracellular ionic composition (Table I, SBIS). In thorough darkness, single cones bathed in normal Ringer's solution (Table I) exhibit a mean holding current at −40 mV of -3.6 ± 5.8 pA ($n = 20$). Illumination suppresses an outer segment inward current that flows through cGMP-gated ion channels; following convention, we define this light-dependent suppression in inward current as an outward photocurrent. As typical of all vertebrate photoreceptors, flash illumination of bass single cones causes a transient photocurrent whose peak amplitude increased with light intensity up to a saturating value (Fig. 1) (Miller and Korenbrot, 1993). Brighter flashes sustain the saturated photocurrent amplitude for ever longer periods of time. The initial time course of saturated photocurrents is well fit by the sum of two, first order exponential processes (Cobbs and Pugh, 1987; Hestrin and Korenbrot, 1990; Perry and McNaughton, 1991). The faster process, time constant of 2.5–5 ms, is light dependent and reflects the

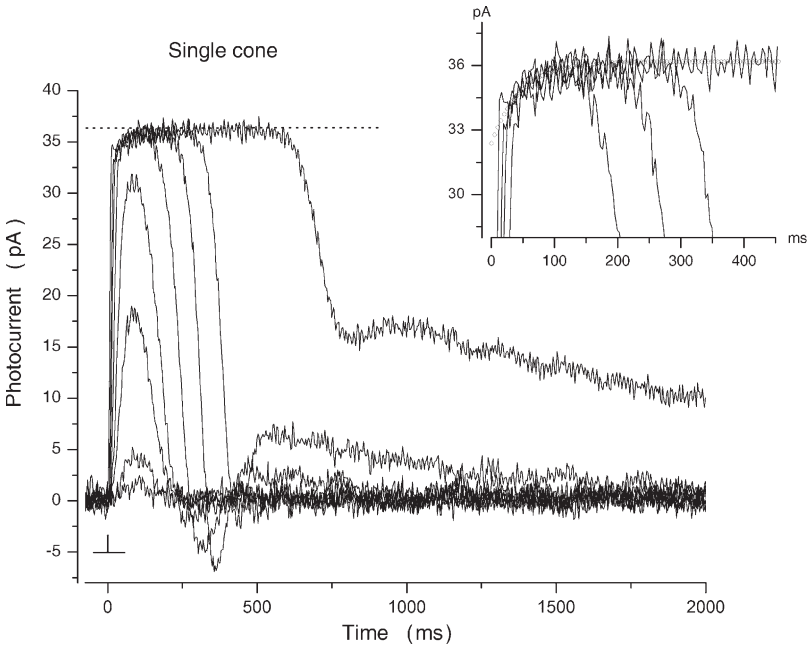

Figure 1. Photocurrents in striped bass isolated single cones. Shown are voltage-clamped currents measured at −40 mV at room temperature. 10-ms flashes of 540-nm light were delivered at time zero. Intensity of the flashes tested was (in photons/μm^2) 0.3, 1.7, 7.8, 44.6, 177.8, 1,071, 4,897, 19,496, and 112,190, respectively. At intensities sufficient to saturate photocurrent amplitude, the current approached saturation along a time course well described by a single first order exponential process (inset, photocurrents generated by the last four flashes). The exponential time course was the same at all intensities tested and was well fit by Eq. 1 with the adjustable values: I_{init} = 32.3 pA, I_{NCKX} = 3.8 pA, and τ_{NCKX} = 46.1 ms.

limiting rate of activation of the enzymes in the phototransduction cascade (Cobbs and Pugh, 1987; Hestrin and Korenbrot, 1990). This fast component, we now know, is more properly described by a Gaussian function (Lamb and Pugh, 1992; Smith and Lamb, 1997). The slower process is insensitive to light and is well fit by the following function (Fig. 1, inset):

$$I_{photo}(t) = I_{init} + I_{NCKX}(1 - \exp(-t/\tau_{NCKX})), \qquad (1)$$

where I_{init} is the amplitude of the photocurrent excluding the exponential component, I_{NCKX} is the maximum amplitude of the exponential component, and τ_{NCKX} is its time constant. The saturated photocurrent amplitude is $I_{sat} = I_{init} + I_{NCKX}$. The mean (±SD) values of these constants were: I_{init} = 27.8 ± 8.6 pA, I_{NCKX} = 2.9 ± 1 pA, and τ_{NCKX} = 62.8 ± 13.5 ms (n = 20 cells). The maximum amplitude of the exponential component is 9.8 ± 2.4% of the maximum photocurrent amplitude.

The slow exponential component in the initial time course of the saturated photocurrents in bass single cones (Fig. 1) is similar to signals previously observed in cones of the tiger salamander retina, and understood to arise from the electrogenic activity of a Na^+/Ca^{2+} exchanger (Nakatani and Yau, 1988; Hestrin and Korenbrot, 1990; Perry and McNaughton, 1991). A diagnostic tool to confirm the functional origin of this exponential component is to characterize the kinetics of the saturated photocurrent in the presence and absence of extracellular Na^+ and Ca^{2+} (Yau and Nakatani, 1985; Hodgkin et al., 1987). If the exponential component arises from Na^+-dependent active Ca^{2+} extrusion, it should disappear when Na^+ is removed from solution because Na^+/Ca^{2+} exchanger activity is absolutely dependent on the presence of Na^+. It is important to replace Na^+ with a cation that permeates through the CNG channels in order to preserve the light-sensitive current. Moreover, extracellular Ca^{2+} must also be removed alongside Na^+ to avoid loading the cytoplasm with Ca^{2+} and, hence, blocking phototransduction (Yau and Nakatani, 1985; Hodgkin et al., 1987). We replaced Na^+ with Li^+ because the permeation properties of both cations through cone CNG channels are nearly the same (Picones and Korenbrot, 1992; Haynes, 1995). Results of such ion substitution test in bass single cones are illustrated in Fig. 2. In normal Ringer's, a bright flash caused a photocurrent that approaches its saturated amplitude with an exponential time course (Fig. 2, A and B), remained saturated for nearly 1 s, and then slowly recovered to its starting value. When Na^+ in the Ringer's was isoosmotically replaced with Li^+ and Ca^{2+} reduced to 1 μM concentration (using the chelator HEDTA), the same flash in the same cell generated a photocurrent that lacked the exponential component at its onset, yet remained saturated and recovered with nearly unchanging features (Fig. 2, C and D). The change in photocurrent kinetics was reversed upon returning to Na^+ Ringer. We made the same observation in every cell tested (n = 6). The reversible loss of the slow exponential component in the saturated photocurrent when extracellular Na^+ and Ca^{2+} are removed demonstrates this component arises from the electrogenic activity of the Na^+/Ca^{2+} exchanger.

Data in Fig. 2 also show that the recovery from photocurrent saturation in cone photoreceptors is generally similar in normal and Li^+, low Ca^{2+} Ringer's. This behavior in bass cones is similar to that reported for tiger

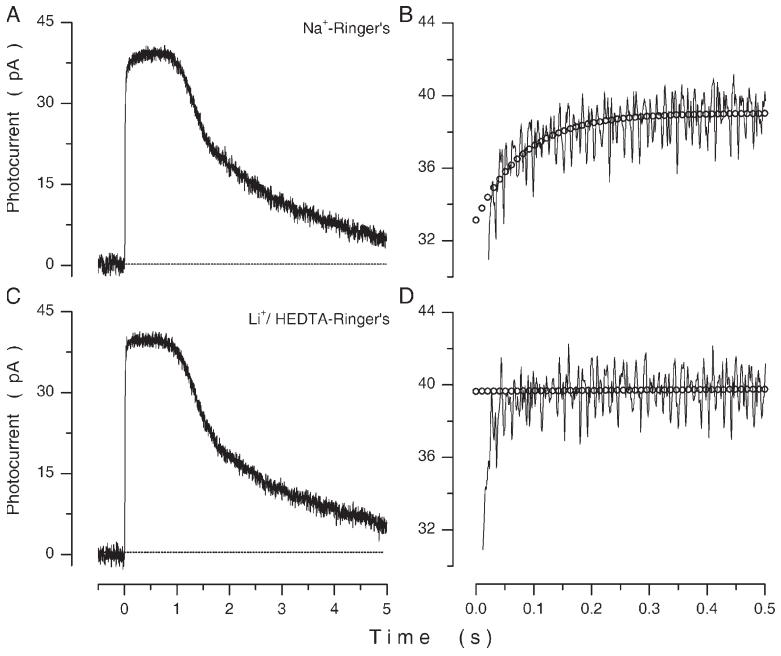

Figure 2. Effects of isoosmotic replacement of extracellular Na^+ with Li^+ on the time course along which bright flash photocurrent approaches amplitude saturation. Shown are voltage-clamped photocurrents measured at −40 mV and elicited by a 1-ms flash of bright white light (intensity: 0.26 nW/μm²). Currents were measured in the same dark-adapted cone both in normal Ringer's solution and in Na^+-free Li^+-Ringer's containing 1 μM free Ca^{2+}. Flashes were delivered 20 s after switching solutions. A and B show the data measured in normal Ringer's displayed at two different temporal resolutions. The photocurrent approaches saturation with an exponential time course well described by Eq. 1 with the adjustable values: I_{init} = 33.1 pA, I_{NCKX} = 5.9 pA, and τ_{NCKX} = 84.4 ms (open circles). C and D show the data measured in Li^+ Ringer's displayed at two temporal resolutions. The photocurrent approached saturation nearly instantaneously without evidence of the slow exponential component. Open circles depict a line optimally fit to the data with slope 0.0002 pA/s.

salamander rods tested under a similar experimental design (Nikonov et al., 1998).

K^+ Dependence of NCKX Current

To determine whether the exchanger in cone photoreceptors is K^+ dependent we examined the ionic properties of the current generated by the exchanger. To better resolve the features of currents generated by the Na^+/Ca^{2+} exchanger (NCKX) we lessened the contribution of other current sources through pharmacological block of several of the voltage- and ligand-gated ion channels expressed in cone photoreceptors (Maricq and Korenbrot, 1988, 1990; Barnes and Hille, 1989). L-type voltage-gated Ca^{2+} channels were blocked with nifendipine (10 μM), and delayed rectifier voltage-gated K^+ channels (IKv) were blocked with intra- and extracellular quaternary amines, TEA and TMA (Table I). We did not block the inward rectifier channels (Ih) to make available an electrical assay of cell integrity but conducted all studies at 0 mV, a voltage at which these channels are inactive. Finally, cells were under constant illumination and the tight seal electrode-filling solution lacked ATP and GTP. These conditions prevent the accumulation of intracellular cGMP and assured that the cell's CNG ion channels were inactive. Currents were measured commencing 3.5–4 min after first attaining whole-cell mode, time sufficient for cell cytoplasm and electrode filling solution to come to equilibrium (Holcman and Korenbrot, 2004).

To characterize the K^+ dependence of the Na^+/Ca^{2+} exchanger, we filled cones with an ionic solution, NCKX-IS (Table I) designed to maintain normal, forward operation of the transporter, except during brief experimental trials when changes in extracellular solutions forced the exchanger to operate in its reverse mode. If the cell-filling solutions did not sustain normal exchanger function, cones filled with Ca^{2+} and did not survive. While loading NCKX-IS, membrane voltage was held at zero; membrane current was initially outward (15–40 pA in amplitude) due to outward K^+ flux through voltage-gated K^+ channels. As contents exchanged/diffused between cell and electrode lumen, these channels were blocked and the current slowly declined to a stationary value reached in ∼3 min. For 41 cells, the mean value of this stationary current at 0 mV was 3.4 ± 7.6 pA (range −10 to 20 pA).

Fig. 3 illustrates typical currents measured in individual single cones starting 3 min after first attaining whole cell mode. Statistical data for the universe of cells studied is detailed in Table III. Switching the extracellular solution from normal Ringer's to a Na^+-free solution containing 0.1 mM Ca^{2+} and Li^+, but no K^+, caused small changes in current that likely arise from changes in junction and tip potentials due to the difference in ionic mobilities of Na^+ and Li^+. The current amplitude in Li^+, absent K^+, was measured in each and every cell studied, and we used this value as a benchmark to define the health of the cells and to compare among them. For 41 cells, this benchmark current at 0 mV holding voltage had a mean value of 5.9 ± 8.3 pA (range −11 to 25 pA). Cell superfusing solution was next switched to a Li^+ solution now containing only 1 μM free Ca^{2+}, 1 mM free Mg^{2+}, and varying test K^+ concentrations. When the K^+ concentration was small (≤10 mM), this solution change caused almost no change in current (Fig. 3 A). At higher extracellular K^+ concentrations, the solution change caused an inward current (Fig. 3 B). This is almost certainly due to inward K^+ flux through

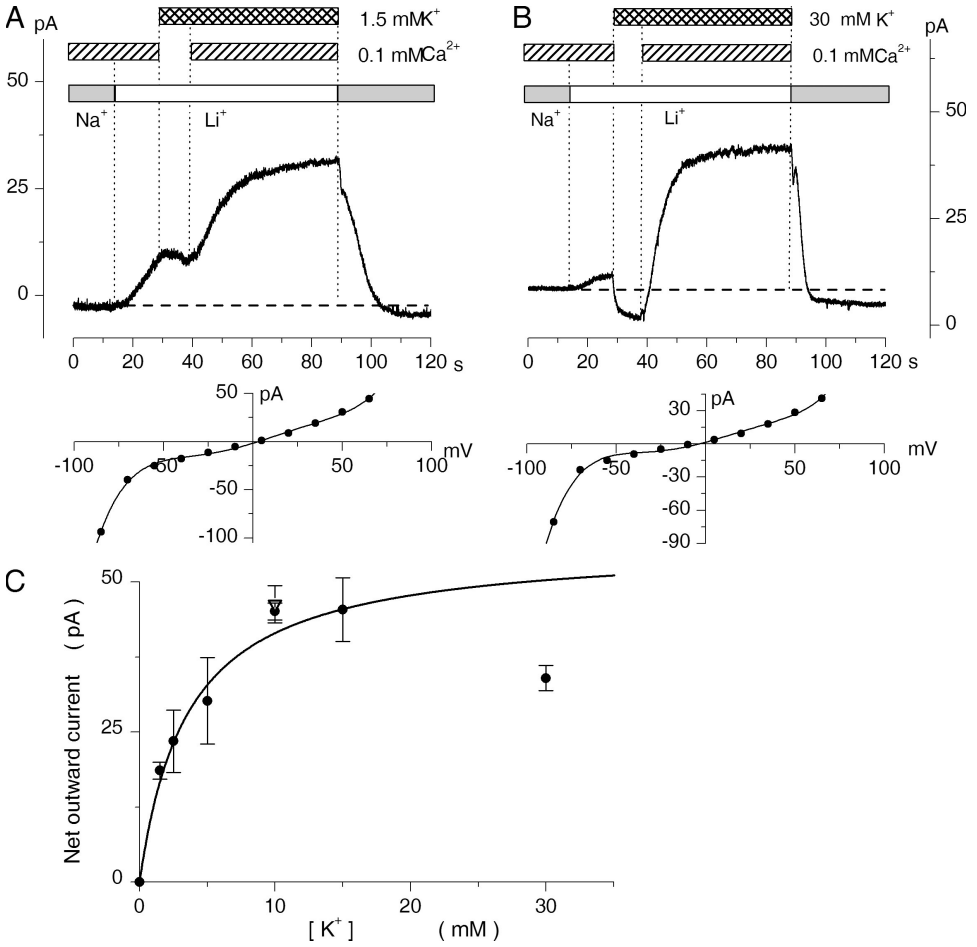

Figure 3. K^+ dependence of outward current generated by the reverse mode operation of Na^+/Ca^{2+}, K^+ exchangers in intact bass single cones. Shown are voltage-clamped membrane currents measured at 0 mV in response to successive changes in extracellular bathing solution. A and B show different cells. The cell in A was bathed in Ringer's that was then successively switched to bathing solutions containing (1) Li^+ (Na^+-free), 0.1 mM Ca^{2+}, K^+-free; (2) Li^+ (Na^+-free), Ca^{2+} free (1 μM), 1.5 mM K^+; and (3) Li^+ (Na^+-free), Ca^{2+} 0.1 mM, and 1.5 mM K^+. Bathing solution was then returned to Ringer's. The cone in B was initially in Ringer's and then switched successively to (1) Li^+ (Na^+-free), 0.1 mM Ca^{2+}, K^+-free; (2) Li^+ (Na^+-free), Ca^{2+}-free (1 μM), 30 mM K^+; and (3) Li^+ (Na^+-free), 0.1 mM Ca^{2+}, and 30 mM K^+. Underneath each current trace is the I-V curve measured for that cell at the end of the trial. In C, filled circles (●) are mean (±SEM) steady-state current amplitude measured in a total of 49 cells filled with NCKX-IS solution at various extracellular K^+ concentrations as the difference before and after the addition of Ca^{2+} (Table I). Also shown as open triangles (▽) is the mean (±SEM) current amplitude of 11 cells filled with NCKX-IS containing 2 mM BAPTA and measured in the presence of 10 mM extracellular K^+. The continuous line is the best fit to the data of Eq. 2 indicating K^+ dependence is well described by the kinetics of binding to a single site of 3.6 mM affinity.

unblocked K^+ channels in the inner segment driven by the favorable inward K^+ concentration gradient. Residual Kv channel activity, despite the presence of blocking quaternary amines in both intra- and extracellular solutions, is evident in the cell's I-V curves; at strong (>40 mV) depolarizing voltages there is a small, but unequivocal, outward rectification (Fig. 3, A and B, I-V curves).

Cell superfusion with solutions now containing 0.1 mM Ca^{2+}, in the continuing presence of Li^+ and K^+, caused a large outward current of amplitude dependent on extracellular K^+ (Fig. 3, A and B). The Ca^{2+}- and K^+-dependent outward current rose relatively slowly and reached a stationary value 10 to 15 s after a solution change. It remained at that value as long as the ionic concentrations remained unchanged (no apparent inactivation) and returned to its starting value when cells were again bathed in normal Ringer's (Fig. 3). The relatively large current and associated cytoplasmic Ca^{2+} load often damaged the cells. To minimize this damage, we tested only a single K^+ concentration on any one cell and completed all trials within 10 min after attaining whole cell mode. We assessed that cells remained healthy by measuring their I-V curve between −85 and 80 mV at the end of the current measurement (Fig. 3). In healthy cells, the curve exhibited strong inward rectification (the activity of Ih channels) and a small outward rectification (unblocked Kv channels). The mean slope resistance between −10 and 5 mV of the cells analyzed here was $2.6 \pm 0.8 \times 10^8\ \Omega$ ($n = 19$, range 1.2 to 4.1×10^8).

The K^+- and Ca^{2+}-dependent outward current we observed in the bass cones are consistent with the electrogenic activity of Na^+/Ca^{2+}, K^+ exchanger operating in its reverse mode; the outward Na^+ concentration gradient (35 mM in/0 out) fuels the active inward flux of Ca^{2+} accompanied by K^+. The relatively slow speed of current activation is probably limited by the velocity of solution exchange near the NCKX molecules, since access to the extracellular surface of the cone outer segment plasma membrane is likely restricted by the characteristic membrane folding of the organelle, especially in nonmammalian species (Fetter and Corless, 1987). When the

TABLE III

Mean Current Amplitude of Reverse Mode NCKX Current in Bass Single Cones

K^+ concentration	Steady-state current amplitude	*n*
mM	*pA*	
0	0	
1.5	18.6 ± 4	9
2.5	23.5 ± 9	4
5	30.2 ± 14.4	5
10	45.1 ± 3.1	6
10[a]	46.3 ± 9.7	11
10[b]	45.9 ± 7.6	6
15	45.4 ± 10.7	5
30	34 ± 5.9	9

[a]Electrode-filling solution contained 2 mM BAPTA titrated to yield 400 nM free Ca^{2+}.

[b]Electrode-filling solution contained 0.1 mM bis-Fura2.

solution is switched back to Ringer's, the exchanger returns to its normal, forward operation. The outward going current is replaced by an inward going current, and Ca^{2+} is transported out from the outer segment (next section), until the cell returns to the initial ionic gradients and its initial Ca^{2+} concentration. We affirmed the K^+- and Ca^{2+}-dependent outward current activated by superfusion and the inward current observed upon returning to Ringer's arises from the electrogenic activity of the NCKX exchanger by demonstrating that the currents are specifically associated with loading and unloading free Ca^{2+} in the cone outer segment (see below).

The amplitude of the NCKX reverse current depended strictly on the presence of extracellular K^+. The mean current amplitude measured in the presence of various K^+ concentrations as the difference before and after the addition of 0.1 mM Ca^{2+} is presented in Table III and Fig. 3. The current amplitude depends on extracellular K^+ in a manner well described by the kinetics of binding to a single site on the exchanger:

$$I_m = \frac{\mathrm{I}_{max}[K]_o}{K_m^K + [K]_o}, \qquad (2)$$

where I_{max} is the maximum possible current, $[K^+]_o$ is the extracellular K^+ concentration, and K_m^K is the binding constant of the single binding site. The adjustable parameters that best fit the mean data of a total of 54 cells (Fig. 3) were I_{max} = 57 pA and K_m^K = 3.6 mM.

Changes in Cytoplasmic Free Ca^{2+} Caused by NCKX Activity

To test the relationship between the K^+- and Ca^{2+}-dependent NCKX current and cytoplasmic free Ca^{2+} levels, we simultaneously measured membrane current and cell fluorescence in bass cone loaded with the indicator dye bis-Fura2 dye (0.1 mM) by diffusion from the tight seal electrode (Table I, solution NCKX-IS with dye).

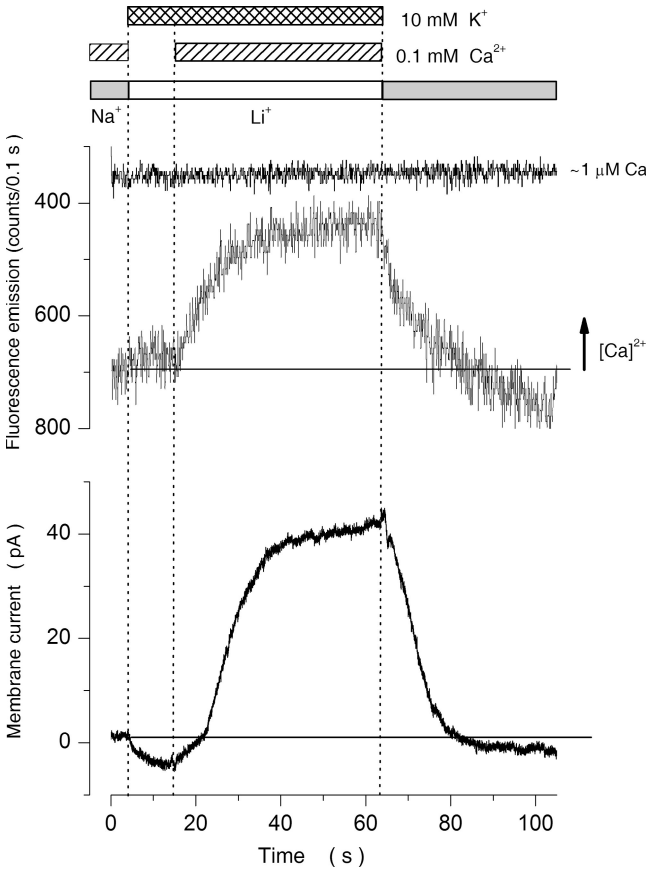

Figure 4. Simultaneous changes in membrane current and cytoplasmic free Ca^{2+} in a single bass cone upon activation of reverse mode Na^+/Ca^{2+}, K^+ transport activity. Shown are voltage-clamped membrane current measured at 0 mV and fluorescence emission intensity of 0.1 mM bis-Fura2 loaded into the isolated cell. Fluorescence was excited at 380 nm and light intensity emitted in the 480–560 nm range measured using photon counting technology (counts/100 ms bin). The solution superfusing the cell was switched from normal Ringer's first to a Na^+-free (Li^+) solution containing 10 mM K^+ and 1 μM Ca^{2+} and then to the same solution now containing 0.1 mM Ca^{2+}. The simultaneous presence of K^+ and Ca^{2+} activated the NCKX transporter in its reverse mode and caused both activation of an outward current and a rise in cytoplasmic free Ca^{2+}. Both current and free Ca^{2+} returned to their starting values after return of the cell to normal Ringer's. The fluorescence emission intensity of bis-Fura2 was not absolutely calibrated in situ, nonetheless, free Ca^{2+} reaches a value of near 1 μM, as revealed by the minimum emission intensity of the dye (the continuous trace), which is attained at ~1 μM free Ca^{2+}.

Cell fluorescence was excited at 380 nm and fluorescence emission intensity measured in the 480–560 nm range. We did not carry out thorough in situ dye calibration and can only report relative, not absolute, changes in Ca^{2+} concentration.

Activation of the reverse mode NCKX transport activity caused simultaneous changes in current and cytoplasmic free Ca^{2+}, as illustrated in Fig. 4. While single cones were bathed in normal Ringer's, the cytoplasmic free Ca^{2+} was fixed and fluorescence emission intensity

TABLE IV

Primers Designed To Identify Specific NCKX Molecular Species as Reaction Products of Two Sequential Nested PCR Reactions

	NCKX2.1	NCKX2.2	NCKX2.3	NCKX2.6	NCKX1
PCR1	SBX3M/SBX2	SBX1/SBX4	SBX5/SBX2	SBX1/SBX4	SBX13/SBX14
PCR2	SBX7M/SBX2	SBX3M/SBX4	SBX7M/SBX2	SBX5/SBX4	SBX13/SBX14
Size amplicon	209 bp	149 bp	209 bp	139 bp	404 bp

constant. Superfusing the cells with a Na^+-free (Li^+) solution with 10 mM K^+ and 1 μM Ca^{2+} caused an inward current with a small change in cytoplasmic Ca^{2+} level. The inward current, as discussed above, reflects inward K^+ flux through unblocked Kv channels. Activation of the reverse mode of NCKX activity by the addition of 0.1 mM Ca^{2+} caused an outward current and a large rise in cytoplasmic Ca^{2+}. Upon returning the cell to normal Ringer's solution, both current and cytoplasmic Ca^{2+} returned to their starting values. We made the same observation in every one of the cells thus tested ($n = 7$). That is, engaging the NCKX exchanger in its reverse mode caused an outward current and cytoplasmic Ca^{2+} loading, returning the exchanger to its normal, forward mode promptly caused an inward current and emptied Ca^{2+} out of the cone outer segment.

The quantitative features of the NCKX reverse mode current in bisFura2-loaded cones were indistinguishable from those observed in the absence of dye and reported above. The benchmark current measured in the Li^+, K^+-free solution had a mean value of 2.3 ± 10.6 pA (six cells), compared with 5.9 ± 8.3 pA in the absence of dye (see above). The maximum outward current, measured as the difference in amplitude in the absence and presence of Ca^{2+} while in the continuous presence of 10 mM K^+, had a mean value of 45.9 ± 7.6 pA (six cells, Table III), again indistinguishable from Fura2-free cells. Indeed, buffering with up to 2 mM intracellular BAPTA did not affect the maximum outward NCKX current in 10 mM K^+ (mean 46.3 ± 9.7, 11 cells, Table III).

The time course of the reverse mode NCKX current is a true measurement of the exchanger activity since one net charge is transported per molecular turnover of NCKX. The change in bis-Fura2 fluorescence, on the other hand, is only an indirect measurement of the exchanger transport because (1) fluorescence emission intensity of bis-Fura2 excited at a single wavelength is not a linear function of Ca^{2+} concentration, and (2) the rate of changes in free Ca^{2+} is affected by intracellular Ca^{2+} buffers of unknown kinetics.

A thorough quantitative examination of the kinetic relationship between NCKX current and cytoplasmic Ca^{2+} is beyond the scope of the work reported here, nonetheless, it is evident that free Ca^{2+} is not simply the integral of the current (as would be expected for passive flux mechanisms, ion channels for example). Rather, both current and Ca^{2+} slowly reach a new steady state after activation of the transporter by the change in superfusing solution (Fig. 4). In the new stationary condition, Ca^{2+} influx (through the active NCKX exchanger) and its efflux from the outer segment (by diffusion into the inner segment and equilibration with the electrode lumen) come to a dynamic balance. At this balance point, Ca^{2+} influx and efflux are the same in magnitude; the net Ca^{2+} flux is zero and the Ca^{2+} concentration is fixed (the fluorescence is constant).

Cloning of Retinal Bass NCKX Exchangers and RT-PCR–based Assignment of Cell of Origin

A bass retinal cDNA phagemid library was screened by hybridization with probes derived from known NCKX mammalian sequences. RACE extension yielded complete, open reading frames of sequences tentatively designated as NCKX1 or NCKX2 by homology with previously known mammalian and avian sequences. NCKX2 exists in four spliced variants NCKX2.1, NCKX2.3, NCKX2.4, and NCKX2.6. Sequences are deposited in GenBank/EMBL/DDBJ under the following accession nos.: bassNCKX1, EF076649; bassNCKX2.1, EF076650; bassNCKX2.2, EF076652; bassNCKX2.3, EF076651; and bassNCKX2.6, EF076653.

To determine the specific cellular origin of the various bass NCKX retinal sequences, we conducted single cell RT-PCR assays of single and twin cones. We collected individual cells and produced cDNA from each one using oligo-dT primers. We followed with two sequential rounds of PCR using primer pairs designed to yield an amplicon if, and only if, a specific NCKX sequence was expressed in the cell under investigation. Table IV lists the primers we used in the first and second round PCR to identify each of the five possible sequences. The cDNA generated from each cell was assayed to assess the expression of every one of the five NCKX sequences in the same cell. PCR products were separated by gel electrophoresis, and detected amplicons were sequenced in both directions using the same primers as in the second round PCR.

For quality control, alongside each cell's reaction we performed positive and negative controls. Positive control, to ensure the cone's mRNA was intact and viable, was to assess the expression of the β subunit of the cGMP-gated ion channel (CNGB3) using protocols and primers described elsewhere (Paillart et al., 2006). Negative control, to ensure only cone specific material was

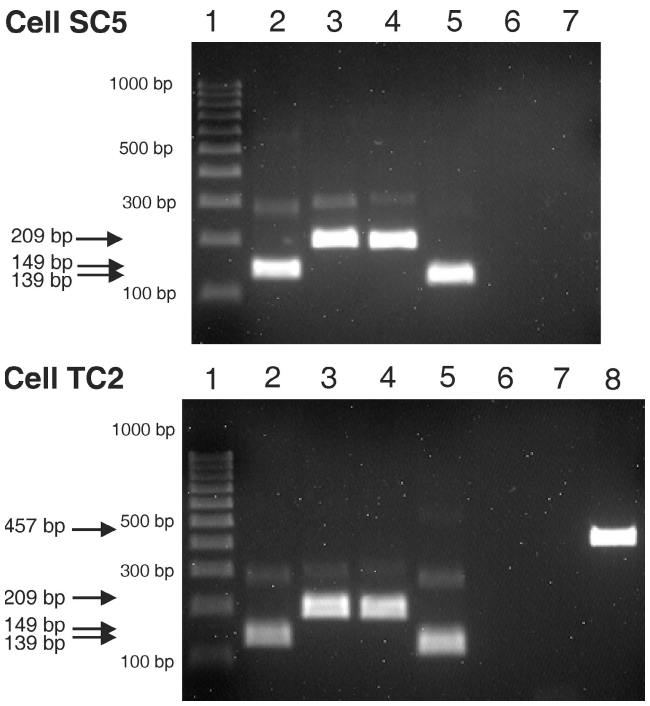

Figure 5. Single and twin cones express each of four splice variants of NCKX2. Images of agarose gel used to characterize reaction products obtained by PCR amplification of single photoreceptor mRNA. Panel SC5 shows the results obtained in one single cone. Panel TC2 shows results in one twin cone pair. cDNA synthesized from individual cells was subjected to two rounds of nested PCR amplification with primer pairs designed to specifically identify the different bassNCKX2 splice variants. Two amplicons were detected with every one of the primer pairs tested. The low abundance amplicon (faint) one is the product of the first round PCR and the abundant one (bright) is produced in the second PCR round. The size and nucleotide sequence of the amplicons indicate that both single and twin cones express each and every one of the four possible splice variants. The primers tested and the expected amplicon sizes were as follows (Tables II and IV): lane 1, 100–1,000-bp standard DNA size markers; lane 2, the photoreceptor tested with primers SBX3M/SBX4, 149-bp amplicon expected for NCKX2.2; lane 3, the photoreceptor tested with primers SBX7M/SBX2, 209-bp amplicon expected for NCKX2.3; lane 4, the photoreceptor tested with primers SBX7M/SBX2, 209-bp amplicon expected for NCKX2.1; lane 5, the photoreceptor tested with primers SBX5/SBX4, 139-bp amplicon expected for NCKX2.6; lane 6, negative control, a sham cell reacted with primers SBX1/SBX2, affirms the absence of relevant DNA contaminants in the bathing solution collected alongside the individual photoreceptor cells; lane 7, negative control, distilled water tested with the same primers as in lane 6, affirms absence of DNA contaminants throughout the sequence of chemical reactions; lane 8, positive control, the photoreceptor tested with primers SB3/SB2 (from Paillart et al., 2006), 457-bp amplicon confirms expression of CNGB3 in the cone.

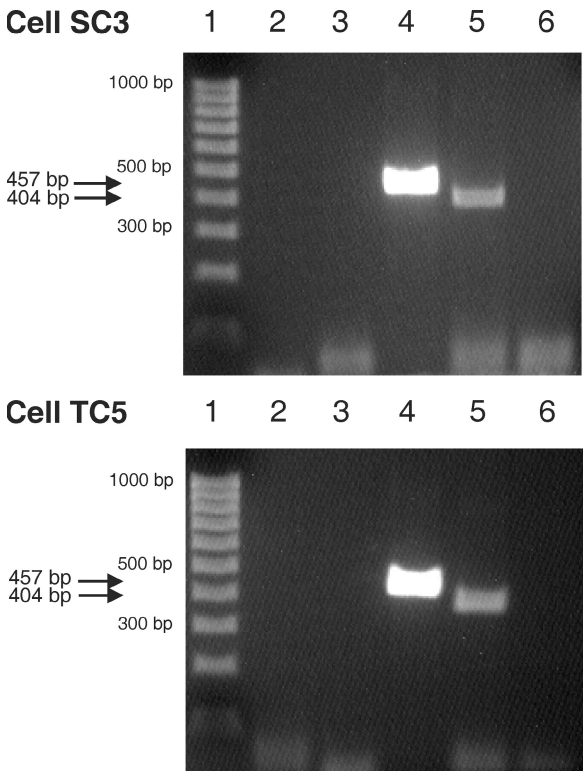

Figure 6. Single and twin cones do not express NCKX1. Agarose gel electrophoresis of reaction products obtained by PCR amplification of single photoreceptor mRNA. Panel SC3 shows results obtained in one single cone. Panel TC5 shows results in one twin cone pair. cDNA synthesized from individual cells was subjected to two PCR rounds of amplification with primer pairs designed to specifically identify bassNCKX1. An NCKX1 amplicon was not detected in either single or twin cones, indicating that cones do not express this molecule. The primers tested and the expected amplicon size were as follows (Tables II and IV): lane 1, 100–1,000-bp standard DNA size markers; lane 2, the photoreceptor tested with NCKX1-specific primers SBX13/SBX14, 457-bp amplicon expected; lane 3, negative control, a sham cell reacted with the same primers as in lane 2, affirms the absence of relevant DNA contaminants in the bathing solution collected alongside the individual photoreceptor cells; lane 4, positive control, the photoreceptor tested with primers SB3/SB2 (from Paillart et al., 2006), 457-bp amplicon, confirms expression of CNGB3 in the cone; lane 5, positive control, cloned bassNCKX1 tested with the same primers as in lane 2, 404-bp amplicon confirms the effectiveness of the PCR reaction to report the existence of NCKX1; lane 6, negative control, distilled water tested with the same primers as in lane 2, affirms the absence of DNA contaminants throughout the sequence of chemical reactions.

amplified, was to assess the expression of the designated NCKX in the cell bathing solution collected in the same volume and in the space where individual cells were gathered. We call this test volume a sham-cell.

Typical electrophoretic analysis of the products generated by two nested, consecutive RT-PCR reactions in individual single and twin cones are illustrated in Figs. 5 and 6. We obtained identical results in the analysis of 10 other single and 8 other twin cones. Fig. 5 A shows an image of a gel used to characterize the reaction products from a single cone using primer pairs designed to assess expression of the four splice variants of NCKX2 (Table IV), alongside positive and negative controls. The controls yielded the required results, indicating that the cell's mRNA was intact and there were no

TABLE V

Features of NCKX-generated Exponential Component in the Initial Rise of Amplitude-saturated Photocurrent

Cones				Rods			
Species	τ_{NCKX}	I_{NCKX}	I_{NCKX}/I_{sat}	Species	τ_{NCKX}	I_{NCKX}	I_{NCKX}/I_{sat}
	ms	*pA*	%		*ms*	*pA*	%
Tiger salamander, *A. tigrinum*	95.4 ± 35[a]	3 ± 2.6	6.1 ± 2.3	Tiger salamander	789 ± 403[c]	3.1 ± 1.7	8.8 ± 3.6
	21 ± 7.9[b]		10.4		720 ± 98[d]	1.5 ± 0.7	6.25 ± 0.8
Striped bass, *M. saxatilis*	62.8 ± 13.5	2.9 ± 1	9.8 ± 2.4	Toad, *B. marinus*	400 ± 100[e]	1.5 ± 0.3	
					580[f]	0.95	
					range 270–740	range 0.76–1.2	
				Gecko, *G. gecko*	470 and 6640[g]		
					240 and 1780[h]		

The parameters listed are defined in Eq. 1. Statistical uncertainty is listed as ±SD.

[a]Hestrin and Korenbrot, 1990.

[b]Perry and McNaughton, 1991.

[c]Cobbs and Pugh, 1987.

[d]Lagnado et al., 1992.

[e]Yau and Nakatani, 1985.

[f]Miller and Korenbrot, 1987.

[g]Gray-Keller and Detwiler, 1994. The sum of two exponential components fits exchanger current more accurately than a single exponential.

[h]Korenbrot, 1995.

reaction products in the medium bathing the cell. Two amplicons were identified as the products of the two rounds of nested PCR: a low abundance one (the rather faint band) at ∼300 bp in size and an abundant one (intense band) of different size depending on the primers used (lanes 2–6). The low abundance amplicon at ∼300 bp is of the size expected as the product of the first PCR round. The abundant amplicon is of the size expected as the product of the second PCR round, one that uses the 300-bp amplicon as its substrate. We sequenced the abundant amplicon and found the sequence to be exactly that anticipated from the ORF cDNA retinal clone. Identical results were obtained in the analysis of the PCR products obtained from individual twin cones (Fig. 5 B). These results demonstrate that both single and twin cones express NCKX2 in all its splice variants. NCKX2, hence, is the K^+-dependent Na^+ for Ca^{2+} exchanger in bass cones and it is the same in single and twin cells.

Fig. 6 shows images of gels used to analyze the RT-PCR reaction products from a single cone or a twin cone analyzed to assess the expression of NCKX1. Also shown are positive and negative control reactions run alongside the cell samples. In both cell types we failed to observe reaction products using specific primer pairs. Positive and negative controls yielded the required reaction products, indicating that mRNA was intact in the cells tested, yet the NCKX1-specific primers did not yield products in either single or twin cones. We obtained the same data in the analysis of two single and two twin cones. The data indicate, then, that bass NCKX1 is not expressed in cone photoreceptors. Given this fact, and the homology of bass NCKX1 to the rod-specific NCKX1 molecules expressed in mammals, we suggest that bass NCKX1 is the K^+-dependent Na^+/Ca^{2+} exchanger in bass rods.

BassNCKX1 and BassNCKX2 Protein

The deduced amino acid sequence of the bass cone NCKX2 exchanger and the bass NCKX1 exchanger are presented in Figs. 7 and 8. The sequences are aligned and compared with those from human and chicken, two species from which both rod and cone exchangers have been cloned and the respective transcripts shown to be present in rod and cone photoreceptors. The conserved, general features of the sequences are annotated in the figure. (1) H0 is present in all sequences as a strongly hydrophobic segment, although its specific amino acid sequence varies. H0 is a cleavable signal peptide important for plasma membrane targeting (Kang and Schnetkamp, 2003). (2) An N-terminal hydrophilic loop follows the H0 hydrophobic segment. This N-terminal loop is poorly conserved among the three species, although all sequences have a cluster of positively charged residues. (3) Two clusters of putative transmembrane segments (H1–H5 and H6–H11) that include residues important for Ca^{2+} binding and K^+ dependence of the exchanger function (Kang et al., 2005a,b). (4) The two clusters are separated by a large hydrophilic loop, likely located in the cytoplasm. This loop in mammalian NCKX1 is larger than that in chicken or bass NCXK1, and larger than the corresponding loop in all NCKX2 molecules cloned to date. Thus, mammalian NCKX1 proteins are larger by ∼500 amino acids than all other NCKX1 and NCKX2. The sequence of the cytosolic loop is poorly conserved among species, but all contain a stretch of acidic residues, immediately preceding H6. (5) The

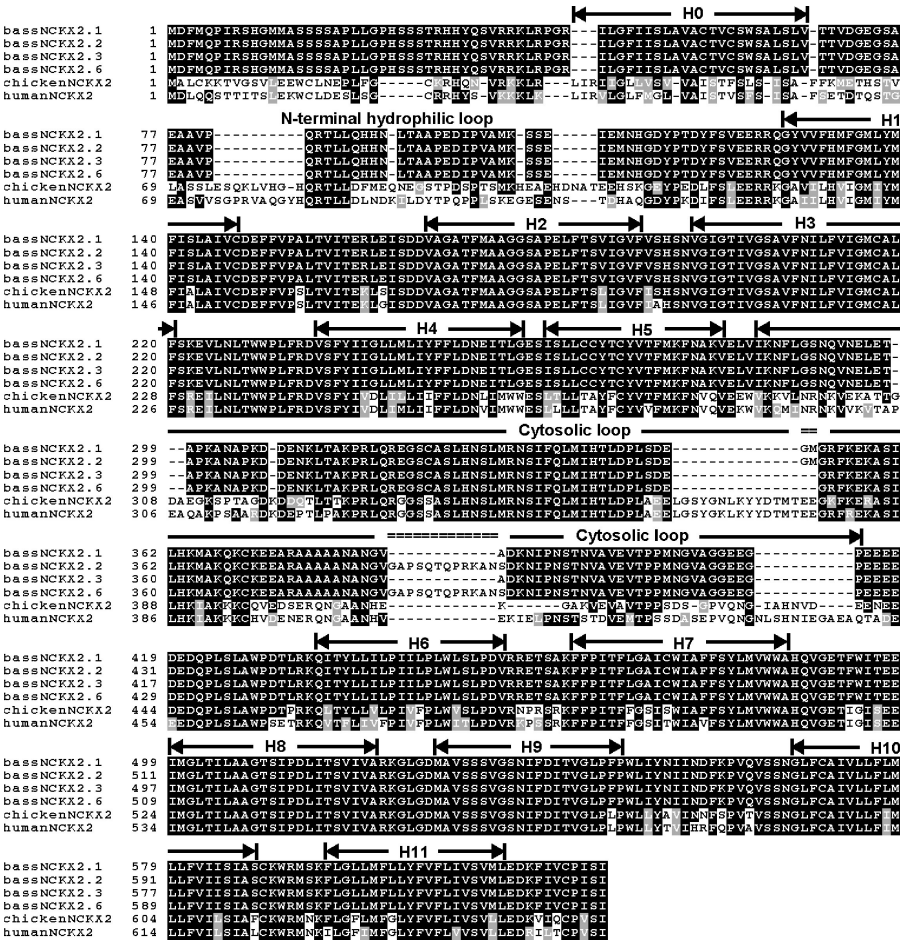

Figure 7. Deduced amino acid sequence of cone-specific bassNCKX2. Aligned are the sequences of the four splice variants of bassNCKX2, alongside the sequences of NCKX2 clones from human and chicken retinas. The major topological features of the proteins' primary structure are identified. H0, a hydrophobic, cleavable signal sequence, a short extracellular loop followed by a cluster of five transmembrane helices (H1–H5). This cluster is separated from a second, similar cluster (H6-H11) by a cytoplasmic loop of variable length and where all the sequence variations are localized (double line).

cytosolic loops of NCKX2 exhibit alternate splicing. Two splice variants have been observed for both chicken and human NCKX2 with the shorter variants lacking the same stretch of 17 residues in the middle of the cytosolic loop. Here, we cloned four distinct splice variants of bass NCKX2 and found transcripts for each variant by single cell RT-PCR. The bass NCKX2 variants all lack the 17-residue stretch found in chicken or human long variants. (6) A short C-terminal loop that is hydrophilic.

DISCUSSION

Active Ca^{2+} efflux from the outer segment of intact bass cone photoreceptors is mediated by a K^+-dependent Na^+/Ca^{2+} exchanger identified here as NCKX2, a member of the NCKX gene family. In darkness, Ca^{2+} is transported out from the outer segment by this exchanger at a rate that balances the passive Ca^{2+} influx through cGMP-gated ion channels, the only ion channels in the outer segment plasma membrane (Yau and Nakatani, 1985; Hodgkin et al., 1987; Miller and Korenbrot, 1987). Bright illumination entirely suppresses the passive Ca^{2+} flux and Ca^{2+} is cleared from the outer segment at a rate determined by the exchanger activity. This clearance rate is controlled by the number and transport rates of NCKX2 molecules, the cytoplasmic free Ca^{2+} concentration, the intracellular K^+ concentration, and the Na^+ ionic gradient. The velocity of Ca^{2+} clearance can be inferred from the slow exponential component observed as the photocurrent reaches amplitude saturation when cones are illuminated with bright light flashes.

Although the time course of this exponential component is frequently taken to be the same as the time course of the light-dependent decline in cytoplasmic free Ca^{2+}, it is not. The actual light-dependent decline in Ca^{2+} concentration is best described by the sum of two exponential components of approximately equal power (in rods, Miller and Korenbrot, 1987; Gray-Keller and Detwiler, 1994; McCarthy et al., 1996; in cones, Sampath et al., 1999). Because of experimental limits imposed by signal to noise ratio, the electrically detectable rate of Ca^{2+} clearance reflects only the faster of the two components. Despite this limitation, electrical measurements in rods and cones of different species (Table V) demonstrate the rate of Ca^{2+} clearance in cones is some 5–10 times faster in cones than in rods, independently of the absolute size of the outer segment or of their membrane surface to outer segment volume ratio.

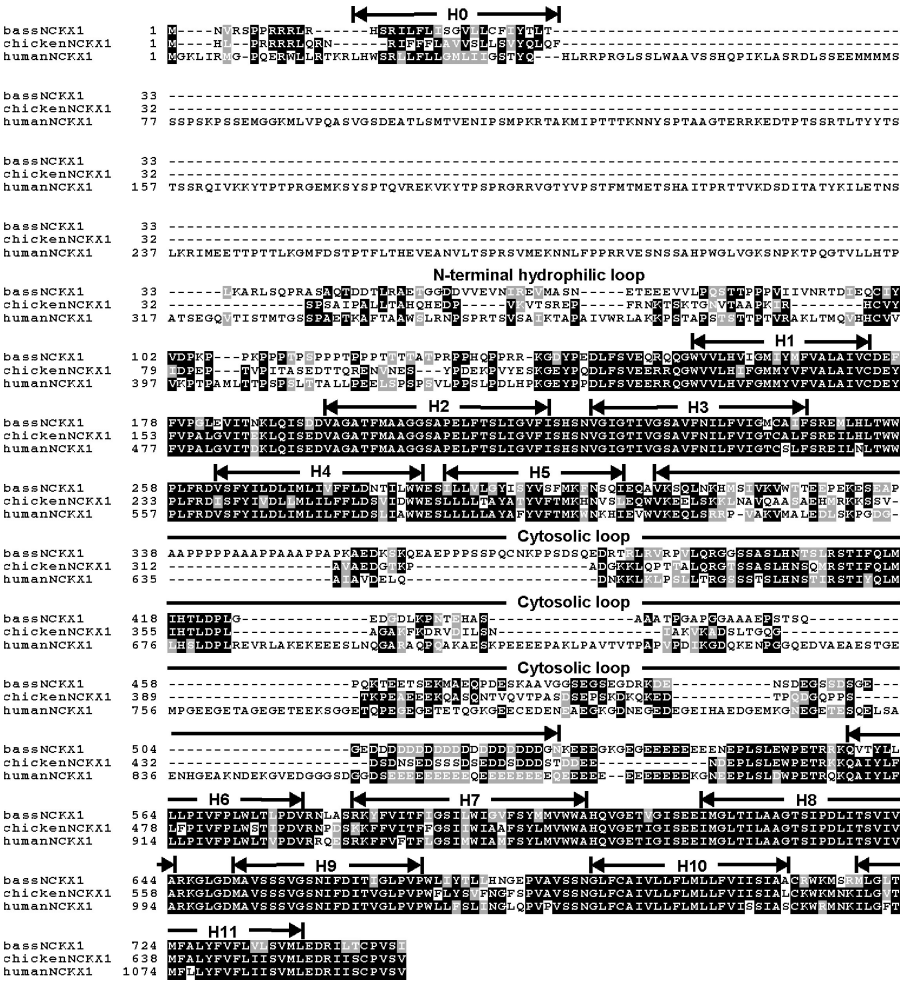

Figure 8. Deduced amino acid sequence of putative rod-specific bassNCKX1. Aligned are the sequences of the bassNCKX1, and NCKX1 clones from human and chicken retinas. The major topological features of the proteins' primary structure are identified. H0, a hydrophobic, cleavable signal sequence, a short extracellular loop followed by a cluster of five transmembrane helices (H1–H5). This cluster is separated from a second, similar cluster (H6–H11) by a cytoplasmic loop of variable length.

The difference in outer segment Ca^{2+} clearance rate between cones and rods contributes to their differences in phototransduction signaling (Rebrik and Korenbrot, 2004), but the mechanism of this difference remains to be understood. Future experiments will address whether the rod/cone difference arises from differences in the packing density and/or transport turnover rates of NCKX1 and NCKX2. While both molecules can be expressed in heterologous cell lines and many of their transport properties have been characterized (Prinsen et al., 2000; Sheng et al., 2000; Dong et al., 2001; Szerencsei et al., 2001), molecular turnover rates are yet to be measured.

The K^+ dependence of NCKX1 and NCKX2 is of great functional significance. Under bright light, Ca^{2+} is transported out of the photoreceptor outer segment by the exchanger molecules until thermodynamic equilibrium is attained. Equilibrium, the condition under which net ion transport by the exchanger stops and, presumably, the condition attained when photocurrent amplitude is saturated is given by (Cervetto et al., 1989)

$$Ca_i = Ca_o \frac{Na_i^4}{Na_o^4} \frac{K_o}{K_i} \exp(V_m F / RT), \quad (3)$$

where Na_i and Na_o are the cytoplasmic and extracellular Na^+ concentrations, Ca_i and Ca_o are the cytoplasmic and extracellular Ca^{2+} concentrations, K_i and K_o are the cytoplasmic and extracellular K^+ concentrations, V_m is membrane voltage, and F, R, and T have their usual thermodynamic meanings. Hence, in a single bass cone, at equilibrium and in normal Ringer's (Table I), cytoplasmic free [Ca_i] can be expected to be 0.04 nM when photocurrent amplitude is saturated at −40 mV. Under identical conditions, a K^+-independent Na^+/Ca^{2+} exchanger can be expected to bring cytoplasmic free Ca^{2+} to only 50 nM. Under comparable ionic conditions, free Ca^{2+} in the outer segment of a tiger salamander cone when photocurrent is saturated is reported to be ∼5 nM (Sampath et al., 1999).

The amplitude of the NCKX current is at its largest value in complete darkness, when Ca^{2+} influx (via CNG channels) is also at its maximum. Under normal ionic gradients, this amplitude is not significantly different in rods and cones, neither in absolute value nor as a fraction of the ionic dark current (Table V). This is not surprising, since the dark current amplitude is also not that different in the two receptor types. Under ionic gradients that engage the reverse mode,

the largest NCKX current amplitude in the bass cones was on average, ~55 pA (Fig. 3). This, again, is not very different than the maximum exchanger current measured in tiger salamander rods (~80 pA, Lagnado and McNaughton, 1991). Finally, the $K_{1/2}$ for K^+ activation in intact bass cones is 3–4 mM, a value well within the range of values of between 1 and 10 mM reported for rods in native membranes (Schnetkamp et al., 1989; Perry and McNaughton, 1993; Rispoli et al., 1995).

Every bass cone we analyzed, whether single or twin, expressed the same four splice variants of bassNCKX2 and did not express bassNCKX1. The unambiguous and simultaneous identification of the four variants required careful design of PCR primers and their use in nested, sequential reactions. The definite identification of the expressed mRNA in individual photoreceptors demanded the synthesis of amplicons of the expected size and a perfect match between their nucleotide sequence and that of the cloned retinal cDNA. Our presumption that bassNCKX1 is an exchanger in bass rods follows from the fact that we only discovered bassNCKX1 and bassNCKX2 in the retina; bassNCKX1 is not in the cones and the nucleotide sequence of bass NCKX1 is homologous to that of other NCKX1 molecules that have been unequivocally shown to be expressed in rods of humans, mice, and chicken. Our inability to do single cell RT-PCR in bass rods does, in a very strict sense, leave the question open as to whether rods in the bass retina may also express NCKX2.

The possibility that more than one molecular isoform is expressed in the same photoreceptor cell is underscored by recent findings on the expression of the visual pigment kinase, identified as GRK1 and GRK7. GRK1 is exclusively found in rods. GRK7 is exclusively expressed in cones of dog and pig retinas (Weiss et al., 2001). However, cones in fish, primates, and humans express both GRK1 and GRK7 (Hisatomi et al., 1998; Weiss et al., 1998; Rinner et al., 2005). A similarly imprecise specificity of expression in rods vs. cones has been described for the family of GCAP proteins, the Ca^{2+}-dependent activators of guanylate cyclase (Imanishi et al., 2004; Palczewski et al., 2004). It might be that the surprising lack of effect on cone transduction signal by knocking out NCKX2 in mice (Li et al., 2006) arises from a lack of evolutionary selection pressure in cones of mice, since mice are a rod-dominated, nocturnal species.

The existence of splice variants of NCKX has been reported before for the rat NCKX1 (Poon et al., 2000) as well as for rat, human, and chicken NCKX2 (Tsoi et al., 1998; Prinsen et al., 2000). The human and chicken splice variants differ in the presence or absence of a 17–amino acid deletion in the cytosolic loop that connects the two sets of transmembrane helices. This 17–amino acid stretch is missing in bass NCKX2, yet splice variants in bass NCKX2 also differ from each other by the amino acid composition of the same cytosolic loop. The functional consequence of the expression of more than one splice variant in bass cones, if any, is to be determined. However, it is unlikely that the function of proteins coded by any one of the four variants differs in their function because the structural differences among them are in a region not known to affect ion transport.

We thank S. Durdam, T. Rebrik, B. Pendergrass, and I. Botchkova for their valuable comments and suggestions.

Olaf S. Andersen served as editor.

Submitted: 17 August 2006
Accepted: 27 November 2006

REFERENCES

Barnes, S., and B. Hille. 1989. Ionic channels of the inner segment of tiger salamander cone photoreceptors. *J. Gen. Physiol.* 94:719–743.

Burns, M.E., and V.Y. Arshavsky. 2005. Beyond counting photons: trials and trends in vertebrate visual transduction. *Neuron.* 48:387–401.

Burns, M.E., and D.A. Baylor. 2001. Activation, deactivation, and adaptation in vertebrate photoreceptor cells. *Annu. Rev. Neurosci.* 24:779–805.

Cervetto, L., L. Lagnado, R.J. Perry, D.W. Robinson, and P.A. McNaughton. 1989. Extrusion of calcium from rod outer segments is driven by both sodium and potassium gradients. *Nature.* 337:740–743.

Chomczynski, P., and N. Sacchi. 1987. Single-step method of RNA isolation by acid guanidinium thiocyanate-phenol-chloroform extraction. *Anal. Biochem.* 162:156–159.

Cilluffo, M.C., H.R. Matthews, S.E. Brockerhoff, and G.L. Fain. 2004. Light-induced Ca^{2+} release in the visible cones of the zebrafish. *Vis. Neurosci.* 21:599–609.

Cobbs, W.H., and E.N. Pugh Jr. 1987. Kinetics and components of the flash photocurrent of isolated retinal rods of the larval salamander, *Ambystoma tigrinum*. *J. Physiol.* 394:529–572.

Cook, N.J., and U.B. Kaupp. 1988. Solubilization, purification, and reconstitution of the sodium-calcium exchanger from bovine retinal rod outer segments. *J. Biol. Chem.* 263:11382–11388.

Cooper, C.B., R.J. Winkfein, R.T. Szerencsei, and P.P. Schnetkamp. 1999. cDNA cloning and functional expression of the dolphin retinal rod Na-Ca+K exchanger NCKX1: comparison with the functionally silent bovine NCKX1. *Biochemistry.* 38:6276–6283.

Dong, H., P.E. Light, R.J. French, and J. Lytton. 2001. Electrophysiological characterization and ionic stoichiometry of the rat brain K^+-dependent Na^+/Ca^{2+} exchanger, NCKX2. *J. Biol. Chem.* 276:25919–25928.

Ebrey, T., and Y. Koutalos. 2001. Vertebrate photoreceptors. *Prog. Retin. Eye Res.* 20:49–94.

Fain, G.L., H.R. Matthews, M.C. Cornwall, and Y. Koutalos. 2001. Adaptation in vertebrate photoreceptors. *Physiol. Rev.* 81:117– 151.

Fetter, R.D., and J.M. Corless. 1987. Morphological components associated with frog cone outer segment disc margins. *Invest. Ophthalmol. Vis. Sci.* 28:646–657.

Gray-Keller, M.P., and P.B. Detwiler. 1994. The calcium feedback signal in the phototransduction cascade of vertebrate rods. *Neuron.* 13:849–861.

Haynes, L.W. 1995. Permeation and block by internal and external divalent cations of the catfish cone photoreceptor cGMP-gated channel. *J. Gen. Physiol.* 106:507–523.

Hestrin, S., and J.I. Korenbrot. 1990. Activation kinetics of retinal cones and rods: response to intense flashes of light. *J. Neurosci.* 10:1967–1973.

Hisatomi, O., S. Matsuda, T. Satoh, S. Kotaka, Y. Imanishi, and F. Tokunaga. 1998. A novel subtype of G-protein-coupled receptor kinase, GRK7, in teleost cone photoreceptors. *FEBS Lett.* 424:159–164.

Hodgkin, A.L., P.A. McNaughton, and B.J. Nunn. 1987. Measurement of sodium-calcium exchange in salamander rods. *J. Physiol.* 391:347–370.

Holcman, D., and J.I. Korenbrot. 2004. Longitudinal diffusion in retinal rod and cone outer segment cytoplasm: the consequence of cell structure. *Biophys. J.* 86:2566–2582.

Imanishi, Y., L. Yang, I. Sokal, S. Filipek, K. Palczewski, and W. Baehr. 2004. Diversity of guanylate cyclase-activating proteins (GCAPs) in teleost fish: characterization of three novel GCAPs (GCAP4, GCAP5, GCAP7) from zebrafish (*Danio rerio*) and prediction of eight GCAPs (GCAP1-8) in pufferfish (*Fugu rubripes*). *J. Mol. Evol.* 59:204–217.

Kang, K., and P.P. Schnetkamp. 2003. Signal sequence cleavage and plasma membrane targeting of the retinal rod NCKX1 and cone NCKX2 Na^+/Ca^{2+}-K^+ exchangers. *Biochemistry.* 42:9438–9445.

Kang, K.J., T.G. Kinjo, R.T. Szerencsei, and P.P. Schnetkamp. 2005a. Residues contributing to the Ca^{2+} and K^+ binding pocket of the NCKX2 Na^+/Ca^{2+}-K^+ exchanger. *J. Biol. Chem.* 280:6823–6833.

Kang, K.J., Y. Shibukawa, R.T. Szerencsei, and P.P. Schnetkamp. 2005b. Substitution of a single residue, Asp575, renders the NCKX2 K^+-dependent Na^+/Ca^{2+} exchanger independent of K^+. *J. Biol. Chem.* 280:6834–6839.

Kim, T.S., D.M. Reid, and R.S. Molday. 1998. Structure-function relationships and localization of the Na/Ca-K exchanger in rod photoreceptors. *J. Biol. Chem.* 273:16561–16567.

Korenbrot, J.I. 1995. Ca^{2+} flux in retinal rod and cone outer segments: differences in Ca^{2+} selectivity of the cGMP-gated ion channels and Ca^{2+} clearance rates. *Cell Calcium.* 18:285–300.

Lagnado, L., and P.A. McNaughton. 1991. Net charge transport during sodium-dependent calcium extrusion in isolated salamander rod outer segments. *J. Gen. Physiol.* 98:479–495.

Lamb, T.D., and E.N. Pugh Jr. 1992. A quantitative account of the activation steps involved in phototransduction in amphibian photoreceptors. *J. Physiol.* 449:719–758.

Li, X.F., L. Kiedrowski, F. Tremblay, F.R. Fernandez, M. Perizzolo, R.J. Winkfein, R.W. Turner, J.S. Bains, D.E. Rancourt, and J. Lytton. 2006. Importance of K^+-dependent Na^+/Ca^{2+}-exchanger 2, NCKX2, in motor learning and memory. *J. Biol. Chem.* 281:6273–6282.

Maricq, A.V., and J.I. Korenbrot. 1988. Calcium and calcium-dependent chloride currents generate action potentials in solitary cone photoreceptors. *Neuron.* 1:503–515.

Maricq, A.V., and J.I. Korenbrot. 1990. Potassium currents in the inner segment of single retinal cone photoreceptors. *J. Neurophysiol.* 64:1929–1940.

McCarthy, S.T., J.P. Younger, and W.G. Owen. 1996. Dynamic, spatially nonuniform calcium regulation in frog rods exposed to light. *J. Neurophysiol.* 76:1991–2004.

Miller, D.L., and J.I. Korenbrot. 1987. Kinetics of light-dependent Ca fluxes across the plasma membrane of rod outer segments. A dynamic model of the regulation of the cytoplasmic Ca concentration. *J. Gen. Physiol.* 90:397–425.

Miller, J.L., and J.I. Korenbrot. 1993. Phototransduction and adaptation in rods, single cones, and twin cones of the striped bass retina: a comparative study. *Vis. Neurosci.* 10:653–667.

Nakatani, K., and K.W. Yau. 1988. Calcium and magnesium fluxes across the plasma membrane of the toad rod outer segment. *J. Physiol.* 395:695–729.

Nakatani, K., and K.W. Yau. 1989. Sodium-dependent calcium extrusion and sensitivity regulation in retinal cones of the salamander. *J. Physiol.* 409:525–548.

Nikonov, S., N. Engheta, and E.N. Pugh Jr. 1998. Kinetics of recovery of the dark-adapted salamander rod photoresponse. *J. Gen. Physiol.* 111:7–37.

Ohyama, T., D.H. Hackos, S. Frings, V. Hagen, U.B. Kaupp, and J.I. Korenbrot. 2000. Fraction of the dark current carried by Ca^{2+} through cGMP-gated ion channels of intact rod and cone photoreceptors. *J. Gen. Physiol.* 116:735–754.

Paillart, C., K. Zhang, T.I. Rebrik, W. Baehr, and J.I. Korenbrot. 2006. Cloning and molecular characterization of cGMP-gated ion channels from rod and cone photoreceptors of striped bass (*M. saxatilis*) retina. *Vis. Neurosci.* 23:99–113.

Palczewski, K., I. Sokal, and W. Baehr. 2004. Guanylate cyclase-activating proteins: structure, function, and diversity. *Biochem. Biophys. Res. Commun.* 322:1123–1130.

Perry, R.J., and P.A. McNaughton. 1991. Response properties of cones from the retina of the tiger salamander JT. *J. Physiol.* 433:561–587.

Perry, R.J., and P.A. McNaughton. 1993. The mechanism of ion transport by the Na^+-Ca^{2+},K^+ exchange in rods isolated from the salamander retina. *J. Physiol.* 466:443–480.

Picones, A., and J.I. Korenbrot. 1992. Permeation and interaction of monovalent cations with the cgmp-gated channel of cone photoreceptors. *J. Gen. Physiol.* 100:647–673.

Poon, S., S. Leach, X.F. Li, J.E. Tucker, P.P. Schnetkamp, and J. Lytton. 2000. Alternatively spliced isoforms of the rat eye sodium/calcium+potassium exchanger NCKX1. *Am. J. Physiol. Cell Physiol.* 278:C651–C660.

Prinsen, C.F., C.B. Cooper, R.T. Szerencsei, S.K. Murthy, D.J. Demetrick, and P.P. Schnetkamp. 2002. The retinal rod and cone Na^+/Ca^{2+}-K^+ exchangers. *Adv. Exp. Med. Biol.* 514:237–251.

Prinsen, C.F., R.T. Szerencsei, and P.P. Schnetkamp. 2000. Molecular cloning and functional expression of the potassium-dependent sodium-calcium exchanger from human and chicken retinal cone photoreceptors. *J. Neurosci.* 20:1424–1434.

Rebrik, T.I., and J.I. Korenbrot. 2004. In intact mammalian photoreceptors, Ca^{2+}-dependent modulation of cGMP-gated ion channels is detectable in cones but not in rods. *J. Gen. Physiol.* 123:63–76.

Rinner, O., Y.V. Makhankov, O. Biehlmaier, and S.C. Neuhauss. 2005. Knockdown of cone-specific kinase GRK7 in larval zebrafish leads to impaired cone response recovery and delayed dark adaptation. *Neuron.* 47:231–242.

Rispoli, G., A. Navangione, and V. Vellani. 1995. Transport of K^+ by Na^+-Ca^{2+}, K^+ exchanger in isolated rods of lizard retina. *Biophys. J.* 69:74–83.

Sampath, A.P., H.R. Matthews, M.C. Cornwall, J. Bandarchi, and G.L. Fain. 1999. Light-dependent changes in outer segment free-Ca^{2+} concentration in salamander cone photoreceptors. *J. Gen. Physiol.* 113:267–277.

Schnetkamp, P.P. 2004. The SLC24 Na^+/Ca^{2+}-K^+ exchanger family: vision and beyond. *Pflugers Arch.* 447:683–688.

Schnetkamp, P.P., D.K. Basu, and R.T. Szerencsei. 1989. Na^+-Ca^{2+} exchange in bovine rod outer segments requires and transports K+. *Am. J. Physiol.* 257:C153–C157.

Schnetkamp, P.P.M. 1989. Na-Ca or Na-Ca-K exchange in rod photoreceptors. *Prog. Biophys. Mol. Biol.* 54:1–29.

Sheng, J.Z., C.F. Prinsen, R.B. Clark, W.R. Giles, and P.P. Schnetkamp. 2000. Na^+-Ca^{2+}-K^+ currents measured in insect cells transfected with the retinal cone or rod Na^+-Ca^{2+}-K^+ exchanger cDNA. *Biophys. J.* 79:1945–1953.

Smith, N.P., and T.D. Lamb. 1997. The a-wave of the human electroretinogram recorded with a minimally invasive technique. *Vision Res.* 37:2943–2952.

Szerencsei, R.T., C.F. Prinsen, and P.P. Schnetkamp. 2001. Stoichiometry of the retinal cone Na/Ca-K exchanger heterologously expressed in insect cells: comparison with the bovine heart Na/Ca exchanger. *Biochemistry.* 40:6009–6015.

Tsoi, M., K.H. Rhee, D. Bungard, X.F. Li, S.L. Lee, R.N. Auer, and J. Lytton. 1998. Molecular cloning of a novel potassium-dependent sodium-calcium exchanger from rat brain. *J. Biol. Chem.* 273:4155–4162.

Tucker, J.E., R.J. Winkfein, C.B. Cooper, and P.P. Schnetkamp. 1998. cDNA cloning of the human retinal rod Na-Ca + K exchanger: comparison with a revised bovine sequence. *Invest. Ophthalmol. Vis. Sci.* 39:435–440.

Weiss, E.R., M.H. Ducceschi, T.J. Horner, A. Li, C.M. Craft, and S. Osawa. 2001. Species-specific differences in expression of G-protein-coupled receptor kinase (GRK) 7 and GRK1 in mammalian cone photoreceptor cells: implications for cone cell phototransduction. *J. Neurosci.* 21:9175–9184.

Weiss, E.R., D. Raman, S. Shirakawa, M.H. Ducceschi, P.T. Bertram, F. Wong, T.W. Kraft, and S. Osawa. 1998. The cloning of GRK7, a candidate cone opsin kinase, from cone- and rod-dominant mammalian retinas. *Mol. Vis.* 4:27.

Yau, K.W., and K. Nakatani. 1985. Light-induced reduction of cytoplasmic free calcium in retinal rod outer segment. *Nature.* 313:579–582.